EMBO Molecular Medicine

Novel APP/Aβ mutation K16N produces highly toxic heteromeric Aβ oligomers

*Daniela Kaden[1,2‡], Anja Harmeier[1†‡], Christoph Weise[1], Lisa M. Munter[1], Veit Althoff[1], Benjamin R. Rost[3], Peter W. Hildebrand[4], Dietmar Schmitz[2,3,5], Michael Schaefer[6], Rudi Lurz[7], Sabine Skodda[8], Raina Yamamoto[9], Sönke Arlt[10,11], Ulrich Finckh[8,11], Gerd Multhaup[1,2,12]**

Keywords: aggregation; Alzheimer disease; amyloid-beta toxicity; APP processing; neprilysin

DOI 10.1002/emmm.201200239

Received June 10, 2011
Revised March 01, 2012
Accepted March 02, 2012

Here, we describe a novel missense mutation in the amyloid precursor protein (APP) causing a lysine-to-asparagine substitution at position 687 (APP770; herein, referred to as K16N according to amyloid-β (Aβ) numbering) resulting in an early onset dementia with an autosomal dominant inheritance pattern. The K16N mutation is located exactly at the α-secretase cleavage site and influences both APP and Aβ. First, due to the K16N mutation APP secretion is affected and a higher amount of Aβ peptides is being produced. Second, Aβ peptides carrying the K16N mutation are unique in that the peptide itself is not harmful to neuronal cells. Severe toxicity, however, is evident upon equimolar mixture of wt and mutant peptides, mimicking the heterozygous state of the subject. Furthermore, Aβ42 K16N inhibits fibril formation of Aβ42 wild-type. Even more, Aβ42 K16N peptides are protected against clearance activity by the major Aβ-degrading enzyme neprilysin. Thus the mutation characterized here harbours a combination of risk factors that synergistically may contribute to the development of early onset Alzheimer disease.

INTRODUCTION

Alzheimer disease (AD) is the most common form of dementia worldwide and usually occurs sporadically. A small percentage of cases are attributable to autosomal dominant inheritance, termed familial AD (FAD). Early onset cases are diagnosed in people younger than 65 (Hardy, 2006). FAD is mostly linked to mutations in the genes encoding the amyloid precursor protein (APP) and the presenilins (PS1 and PS2; Kennedy et al, 2003). Recently the first recessive mutation was described in APP causing AD only in homozygous carriers (Di Fede et al, 2009). According to the amyloid hypothesis the main culprits of the disease are amyloid-β (Aβ) peptides, which are generated by the sequential cleavage of APP through β- and γ-secretases (Hardy & Selkoe, 2002; Fig 1A). In contrast, Aβ formation is prevented by α- and γ-secretase proteolysis (Selkoe, 2001b; Fig 1A). Whereas, Aβ40 is the major form in the brain, especially Aβ42 oligomers are suspicious to cause neuronal toxicity and cognitive decline (Chen & Glabe, 2006; Klein et al, 2001; Selkoe, 2001a; Walsh et al, 2002; Younkin, 1998). In addition, it has been assumed that a change in the $A\beta_{42}/A\beta_{40}$ ratio in favour of Aβ42 is causative for the pathology (Kuperstein et al, 2010).

(1) Institut fuer Chemie und Biochemie, Freie Universitaet, Berlin, Germany
(2) Cluster of Excellence NeuroCure, Charité-Universitaetsmedizin Berlin, Berlin, Germany
(3) Neurowissenschaftliches Forschungszentrum, Charité, Berlin, Germany
(4) Institut fuer Medizinische Physik und Biophysik, Charité, Berlin, Germany
(5) DZNE – German Center for Neurodegenerative Diseases, Berlin, Germany
(6) Medizinische Fakultaet der Universitaet Leipzig, Rudolf-Boehm-Institut fuer Pharmakologie und Toxikologie, Leipzig, Germany
(7) Max Planck Institute for Molecular Genetics, Berlin, Germany
(8) Neurologische Universitaetsklinik, Knappschaftskrankenhaus, Universität Bochum, Bochum, Germany
(9) Medizinisches Versorgungszentrum Dortmund Dr. Eberhard & Partner, Dortmund, Germany
(10) University of Hamburg Medical Center Department of Psychiatry and Psychotherapy, Hamburg, Germany
(11) Alzheimer Research Group Hamburg, Hamburg, Germany
(12) Department of Pharmacology & Therapeutics, McGill University, Montreal, QC, Canada
Corresponding author: Tel: +1 514 398 3621; Fax: +1 514 398 2045; E-mail: gmulthaup@me.com
† Present address: Neuroscience Research, Pharmaceuticals Division, F. Hoffmann-La Roche Ltd., Basel, Switzerland.
‡These authors contributed equally to this work.

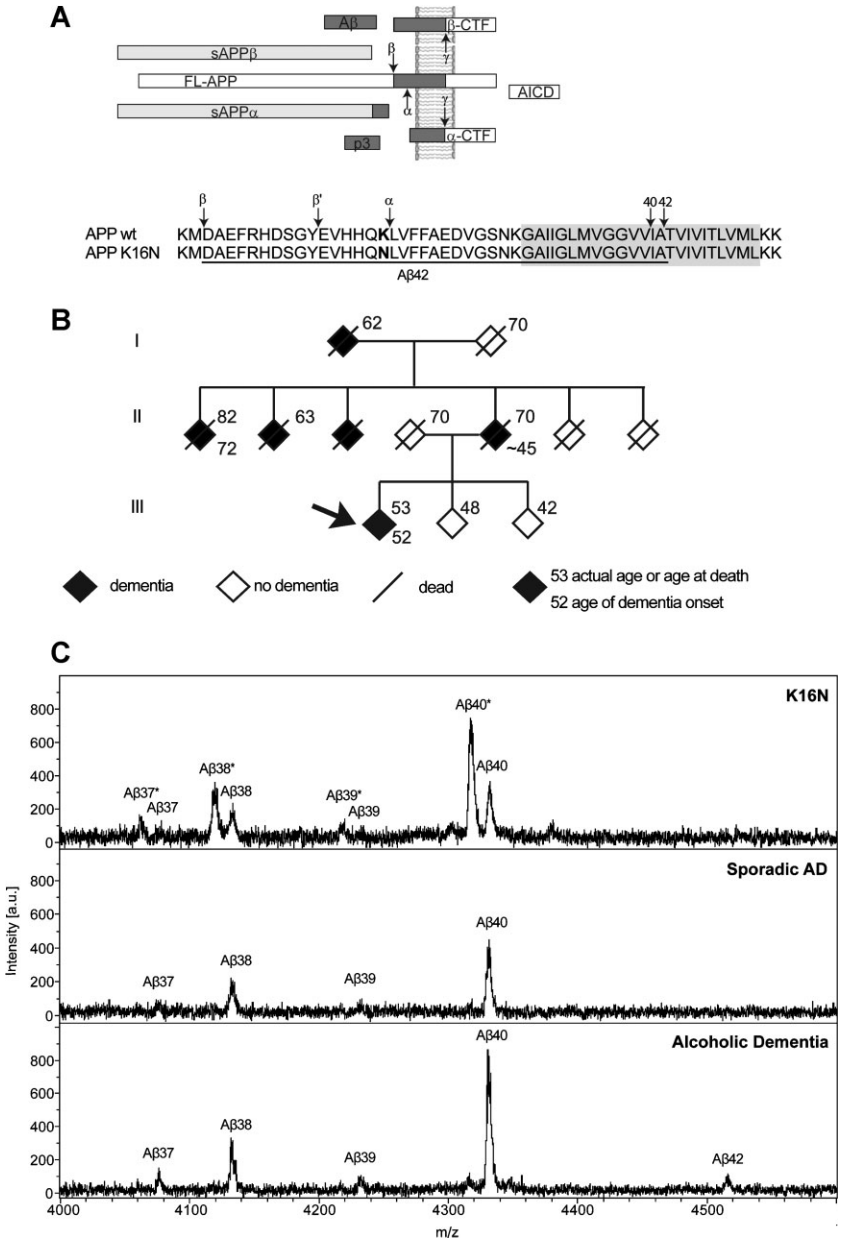

Figure 1. Pedigree of the patient and mass-spectrometry analysis of mutant and wt Aβ in the patient's CSF.

A. Schematic of APP processing. FL-APP is initially cleaved by either the α- or β-secretase. The remaining membrane-bound C-terminal fragments α-CTF and β-CTF, respectively, are further cleaved by the γ-secretase to generate the APP intracellular domain (AICD) and p3 or Aβ. Aβ region is shown in grey. Part of the APP sequence highlighting the Aβ42 region (underlined). The mutation at the α-secretase cleavage site changes the lysine in position 687 of APP (according to APP770 numbering) or position 16 of Aβ to asparagine. Known secretase-cleavage sites are marked by arrows. β′ is an alternative β-secretase cleavage site.

B. Three-generation pedigree of the family. The index patient is marked with an arrow. Four of six siblings of generation II suffered from dementia. Siblings of the index patient have no dementia and have not been tested for the mutation.

C. Aβ from the patient's CSF was precipitated with the monoclonal antibody WO-2 and Aβ masses were determined by MALDI-MS. In CSF of the patient with the K16N mutation a mass shift of 14 Da was detected between wt and mutant Aβ, indicated as Aβ37/38/39/40 (wt) and Aβ37/38/39/40* (K16N). Only in the CSF from the patient suffering from alcoholic dementia Aβ42 was detected. See Table S2 of Supporting Information for the experimental and theoretical masses.

FAD mutations localized to the central hydrophobic core of Aβ peptides [Dutch (E22Q), Flemish (A21G), Italian (E22K), Arctic (E22G) and Iowa (D23N)] enhance toxicity and aggregation propensity of the amyloidogenic peptides (Kumar-Singh et al, 2002; Murakami et al, 2002; Nilsberth et al, 2001; Van Broeckhoven et al, 1990; Van Nostrand et al, 2001). Additionally, two of these mutations – Flemish (A21G) and Arctic (E22G) – which are located in close proximity to the α-secretase cleavage site (K16/L17), diminish non-amyloidogenic processing and increase Aβ levels (De Jonghe et al, 1998; Haass et al, 1994; Sahlin et al, 2007; Stenh et al, 2002).

In the brain several proteases are known to be involved in the clearance of Aβ peptides with neprilysin (NEP) being one of the most extensively studied enzymes (Howell et al, 1995; Iwata et al, 2004; Kanemitsu et al, 2003; Shirotani et al, 2001). This was demonstrated through genetic ablation of NEP causing elevated endogenous Aβ levels (Iwata et al, 2001). NEP is a membrane-bound zinc-metallopeptidase which acts on hydrophobic residues preferentially of oligopeptides such as Aβ (Carson & Turner, 2002). Resistance to NEP-mediated proteolysis might even be a pathogenic mechanism in AD since Flemish mutant (A21G) peptides are degraded significantly slower than Aβ wt (Betts et al, 2008).

Here, we have characterized the first mutation exactly localized to the α-secretase cleavage site (APP_{770}K687N/AβK16N) which causes early onset dementia. The mutation severely affects APP processing, changes the toxic behaviour of Aβ and modulates NEP-mediated degradation of Aβ42. The

non-amyloidogenic cleavage and, therefore, the amounts of α-CTF and the neuroprotective sAPPα were significantly diminished, whereas, unexpectedly both Aβ40 and Aβ42 levels were found increased. Most importantly, the Aβ42 K16N peptide alone is almost non-toxic and only gains severe toxicity when it is mixed with its wild-type (WT) counterpart.

RESULTS

Anamnesis of the index patient carrying the K16N mutation

We have identified a novel heterozygous APP missense mutation at the exact α-secretase cleavage site in a 53-year-old patient with early onset dementia. The mutation consists of an A-to-T transversion of the last nucleotide of the penultimate codon of exon 16 and results in a lysine-to-asparagine substitution at position 687 of APP770 (herein, referred to as K16N according to Aβ numbering; Fig S1 of Supporting Information; Fig 1A). The mutation did not appear in 500 healthy individuals. No further mutation was found in APP (exons 16 and 17), PSEN1, PSEN2 or PRNP of the patient, whose APOE genotype was ε2/ε3. The patient presented with progressive cognitive deficits of various modalities, including dyscalculia, decline of short-term memory, verbal fluency and abilities of visual construction. Cognitive decline was confirmed by DemTect neuropsychologically (Kalbe et al, 2004) after a 3-month interval. MRI analysis revealed mild global brain atrophy without focal or vascular lesions (data not shown). Repeated cerebrospinal fluid (CSF) analysis within a time interval of 8 months suggested Alzheimer-type neurodegeneration with elevated total tau, phospho-tau and reduced Aβ1–42 levels (Table S1 of Supporting Information). Family history is highly suggestive of autosomal dominant early onset dementia (Fig 1B). Samples of other relatives were unfortunately not accessible for evaluation. MALDI-MS analysis of total Aβ immunoprecipitated from the CSF of the patient, another patient with a sporadic AD (74-year old) and a third one with alcoholic dementia (74-year old) revealed an Aβ pattern known from the literature to occur in the human CSF (Fig 1C; Portelius et al, 2006). Additional peaks displaying a mass shift of 14 Da, reflecting the substitution of lysine (K) by asparagine (N), were detected in the K16N patient (Fig 1C). The mass-spectrometry analysis of CSF confirmed the expression of the mutated allele and visualized the heterozygous state on the protein level. Thus, mutant and wt APP derived from the two different alleles are subject to amyloidogenic processing.

Processing of APP K16N

In order to investigate if the mutation causes alterations in the processing of APP, we expressed APP K16N in HEK293 (Fig 2) and SH-SY5Y cells (Fig S2 of Supporting Information). First, we carried out confocal laser scanning microscopy and fluorescence resonance energy transfer (Kaden et al, 2009; Munter et al, 2007) and excluded an aberrant subcellular localization or dimerization behaviour of the mutant full-length APP (FL-APP) compared to the WT (Fig S3 of Supporting Information). Second, we investigated the processing of APP. By Western blot analysis we found the overall amount of secretory APP (sAPPtotal) and particularly sAPPα, drastically decreased (Fig 2A; Fig S2B of Supporting Information). Quantification of sAPPα levels by enzyme-linked immunosorbent assay (ELISA) revealed a 40–50% decrease for APP K16N as compared to APP wt (Fig 2B; Fig S2A of Supporting Information). We additionally analysed sAPPα levels by using the 4B4 antibody (Kuhn et al, 2010) because the W0-2 antibody not only recognizes sAPPα but also sAPPβ′, an alternative β-secretase cleavage product (Yang et al, 2004; Fig 1A). The results of the Western blot and ELISA obtained with W0-2 were, thereby, corroborated (Fig 2A–D). Moreover, sAPPβ levels were found reduced by about 50% (Fig 2C and D). The Western blot analysis of whole cell lysates demonstrated a higher amount of mature APP K16N (Fig 2A; Fig S2B of Supporting Information). In line with this data, analysis of biotinylated plasma-membrane APP showed an increased amount of the mature mutant protein at the cell surface (Fig S4A of Supporting Information). A possible explanation was provided by experiments using the protein synthesis blocker cycloheximide (CHX) which in combination with inhibitors for α- and β-secretase revealed that APP wt has a higher turnover rate than APP K16N (Fig S4B of Supporting Information). Whereas, almost no mature APP wt remained after 4 h of incubation with CHX, APP K16N shows the typical band pattern of mature APP (Fig S4B of Supporting Information). We propose that the higher levels of the mature mutant APP are mainly attributable to a prolonged half-life enabled by reduced ectodomain shedding. Although APP K16N processing was slowed down in general, the levels of Aβ40 K16N and Aβ42 K16N were increased by about 50% as detected by ELISA (Fig 2B; Fig S2A of Supporting Information). Regarding the reduced ectodomain shedding this result encouraged us to analyse the C-terminal fragments (CTFs) which are the direct substrates of the γ-secretase complex and counterparts of ectodomain shedding. CTFs were analysed by immunoprecipitation of cell lysates followed by Western blot analysis. In analogy to the 40–50% reduced sAPPα levels generated from APP K16N, we found the α-CTF levels also strongly decreased (Fig 2E). Densitometric quantification revealed that α-CTF levels of APP K16N were diminished by 75% and β-CTF levels were increased twofold (Fig 2F). That is in contrast to the 50% reduced sAPPβ levels (Fig 2C and D). This observation can be explained as WT β-CTF is not only cleaved by the γ-secretase complex but also N-terminally trimmed by the α-secretase, thereby, producing α-CTF (Kuhn et al, 2010). Thus the diminished amount of α-CTF and the increased β-CTF K16N levels are most likely the result of a strongly reduced α-secretase cleavage caused by the K16N substitution. This increases the available amount of β-CTF as a substrate for γ-secretase cleavage and, thereby, explains the drastically increased generation of Aβ40 and Aβ42 (Fig 2B). Moreover, APP K16N shows an additional band migrating between α-CTF and β-CTF. The detection by C-terminal specific antibodies indicates that this fragment must be an alternative cleavage product which is N-terminally truncated. This view is further supported by MALDI-MS analysis of Aβ precipitated from conditioned media

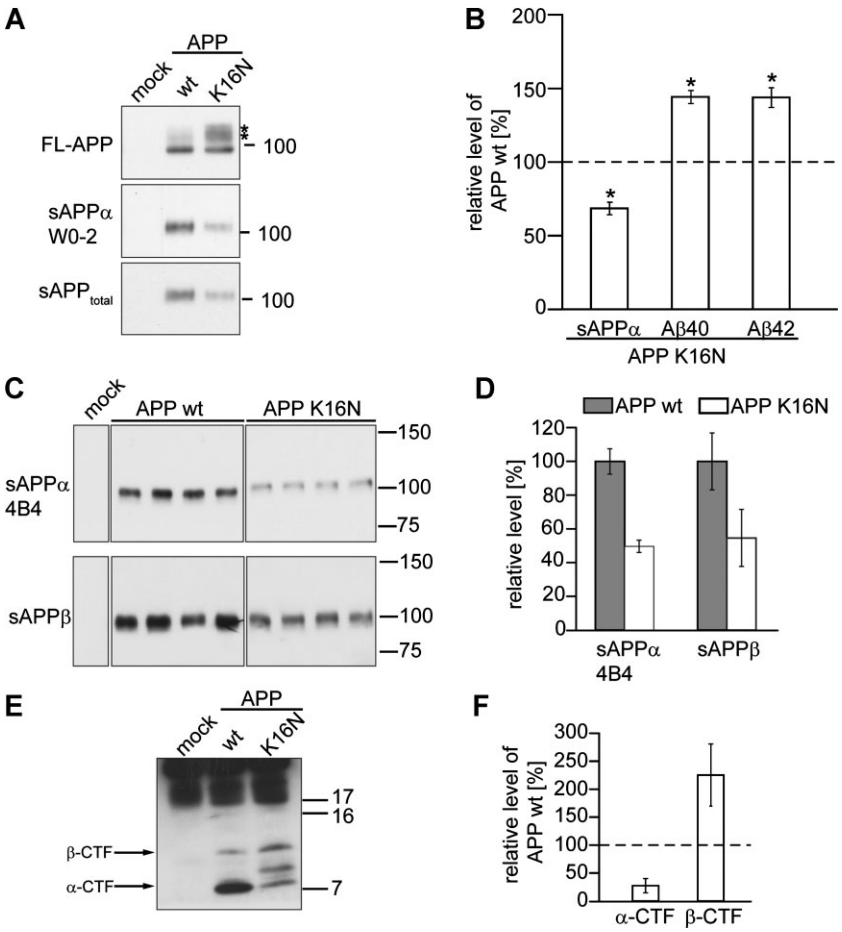

Figure 2. Processing of the mutant APP in HEK293 cells.

A. Representative Western blots of FL-APP (mature forms are marked with *) and soluble APP ($sAPP_{total}$). FL-APP and $sAPP_{total}$ were detected with the myc- and sAPPα by W0-2 antibody. The empty vector (mock) was used as a control.

B. Quantification of sAPPα, Aβ40 and Aβ42 levels by ELISA. Shown are the respective levels of proteolytic fragments normalized to 100% of APP wt ($n = 4 \pm$ SEM). Asterisks indicate significant differences between mutant and wt APP ($^*p < 0.05$ one-way ANOVA followed by posthoc Dunnett).

C. Representative Western blots of sAPPα detected with the 4B4 antibody (Kuhn et al, 2010) and sAPPβ detected with the anti-sAPPβ antibody (IBL).

D. Densitometric quantification of sAPPα and sAPPβ levels from Western blot analysis (five-independent Western Blots with 4–6 samples each).

E. Representative Western blot of APP-CTFs. Lysates were subjected to immunprecipitation and analysed by an APP-C-terminal antibody.

F. Densitometric quantification of the levels of α-CTF and β-CTF from Western blot analysis. Shown are the respective levels of CTFs normalized to 100% of APP wt ($n = 3$).

showing an increased amount of Aβ5–40 derived from APP K16N (Fig S5 and Table S3 of Supporting Information).

Our data indicates that APP K16N is a poor substrate for α-secretase mediated cleavage. However, to clarify whether the poor cleavage is the result of the amino-acid exchange at the α-secretase cleavage site or attributable to other factors, we analysed α-secretase cleavage *in vitro*. Because ADAM10 is known to be the physiologically relevant α-secretase (Kuhn et al, 2010) we used human ADAM10 as protease and the synthetic peptide Aβ11–28 as substrate. The generated fragments were analysed by MALDI-MS. For Aβ11–28 wt the expected proteolytic fragments Aβ11–16 and Aβ17–28 were easily detectable after 3 h (Fig 3A). After 24 h incubation time the substrate Aβ11–28 wt was completely degraded. As a control we used trypsin which generated the fragments Aβ11–16 and Aβ17– 28 after 3 h incubation time (Fig 3A). Since the sequence Aβ11–28 K16N does not contain residues where trypsin could cleave, it was expected not to be a substrate. Indeed, even after prolonged incubation time no fragments could be detected and undigested peptide was still present (Fig 3B). Using ADAM10, however, we observed cleavage of Aβ11–28 K16N even though at a slow rate. After 5 h only small peaks representing the fragments Aβ11–16 K16N and Aβ17–28 were measureable, indicative of slow proteolysis in comparison to the WT (Fig 3B; Fig S6 of Supporting Information). The signal of Aβ11−16 and Aβ17–28 K16N peptides steadily increased over 24 h, although, significant amounts of undigested peptide remained (Fig 3B; Fig S6 of Supporting Information). To compare the effect of APP K16N with other FAD mutations we utilized the arctic mutation E22G which is located close to the α-secretase cleavage site. The arctic mutation leads to reduced sAPPα levels (Stenh et al, 2002). Aβ11–28 E22G is a substrate of trypsin and ADAM10 and completely cleaved after 3 and 24 h incubation time, respectively (Fig 3C). Therefore, reduced α-cleavage of the arctic mutant is not due to the amino-acid substitution but most likely attributable to increased intracellular localization which makes it less available to the α-secretase (Sahlin et al, 2007). In conclusion this data indicates that the K16N amino-acid substitution renders the mutant APP directly a poor substrate of ADAM10 in cell culture and *in vitro*. The reduced cleavage of β-CTF by the α-secretase might be one important cause of the increased Aβ levels. In addition, on the product level the mutant peptides might be more stable against degradation by proteases involved in Aβ clearance. This has been observed for other Aβ peptides with FAD mutations near the α-secretase cleavage site (Betts et al, 2008; Morelli et al, 2003). Since the five known intra-Aβ point mutations located within the hydrophobic core were reported to affect peptide aggregation, toxicity and fibril

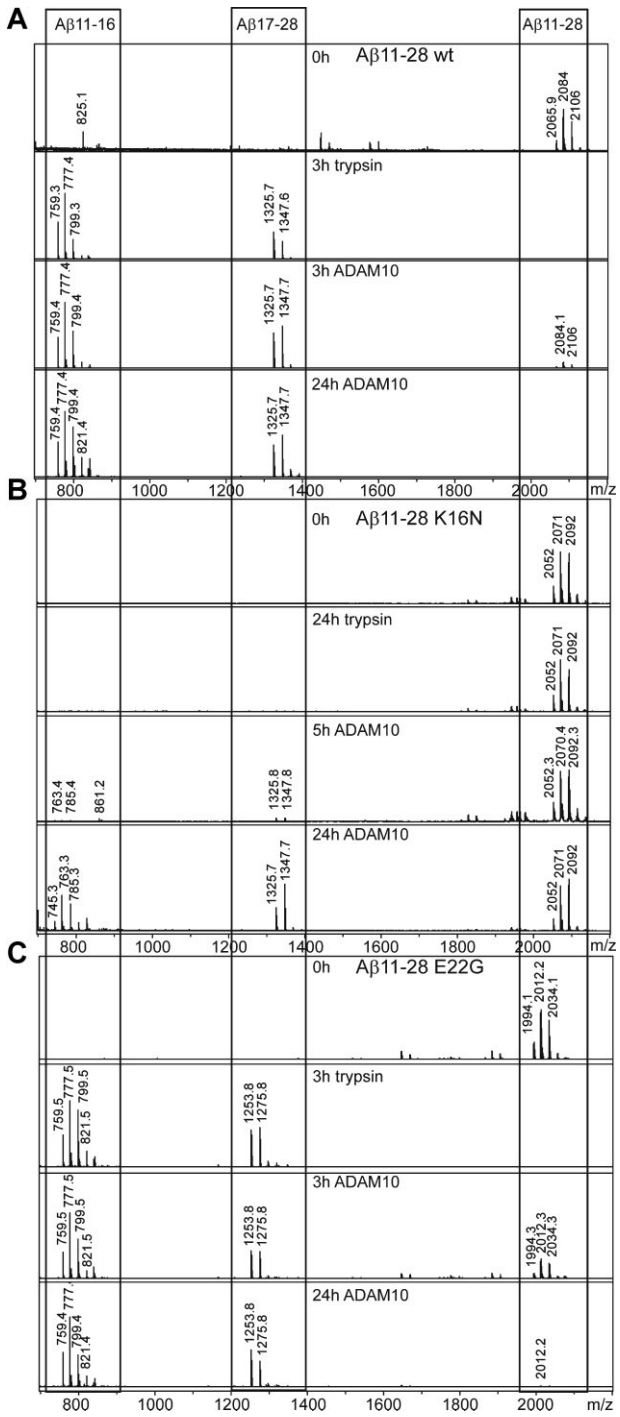

Figure 3. *In vitro* α-secretase (ADAM10) assay.

A-C. Mass spectra of trypsin and ADAM10 proteolysis of Aβ11–28 peptides: wt (**A**), K16N (**B**), E22G (arctic) (**C**). Peptides were incubated for the indicated times with ADAM10 or trypsin and mixed with α-cyano-4-hydroxycinnamic acid matrix and analysed by MALDI-MS. Peptide identities are indicated at the top. See Figure S6 and Table S4 of Supporting Information for details and the experimental and predicted masses. Note, Aβ11–28 K16N is not cleaved by trypsin and cleavage by ADAM10 is significantly slowed down.

formation *in vitro* (Betts et al, 2008; Murakami et al, 2002), these properties were analysed with synthetic peptides carrying the K16N substitution.

Aggregation, toxicity and stability of the Aβ K16N peptide

To elucidate whether the substitution has any effects on early phases of the peptide aggregation, we carried out size exclusion chromatography (SEC) of synthetic Aβ40 wt and Aβ42 wt peptides and the corresponding K16N peptides. Since the patient is heterozygous for the K16N mutation we also analysed the equimolar mixtures of both peptides (Aβ mix). Aβ40 wt, Aβ40 K16N and Aβ40 mix mainly formed low-*n* oligomers (4–6*x*) but no higher aggregates (Fig 4A). Aβ42 K16N predominantly assembled in low-*n* oligomers like the Aβ42 wt peptide (Fig 4B). However, the equimolar mixture of Aβ42 wt and Aβ42 K16N revealed considerably higher amounts of high-*n* oligomers (16–20*x*) at the expense of hexa- and tetramers (Fig 4B, red line). This is in contrast to the recessive A673V mutation, where the mixture of the Aβ40 wt and Aβ40 mutant peptides prevents the formation of low-*n* oligomers while the monomer was stabilized (Di Fede et al, 2009).

Toxicity of the freshly dissolved (load) and SEC-purified Aβ peptides was determined in SH-SY5Y cells (Fig 4C and D). Whereas, other known intra-Aβ mutations increase Aβ-mediated toxicity, Aβ42 K16N peptides were significantly less harmful to neuroblastoma cells than Aβ42 wt (Fig 4D, load). However, severe toxicity of the mutated peptide was gained when mixed with the Aβ42 wt peptide (mix) which then displayed toxicity like Aβ42 wt alone (Fig 4D, load). Dissecting the toxicity of the different oligomers as separated by SEC, mixed Aβ42 16–20-mers induced a massive loss of cell viability, which is in sharp contrast to the almost non-toxic pure Aβ42 wt high-*n* oligomers (Fig 4D). Aβ42 hetero-hexamers maintained the potentiated toxicity, although, the effect was weakened. Low-*n* Aβ42 oligomers (tetramers and dimers) of the mixture were as deleterious as the WT (Fig 4D). Besides the damaging effects of these Aβ42 oligomers, even the usually non-toxic Aβ40 peptide reached significant toxicity when mutant and WT peptides were combined (Fig 4C). Similar to Aβ42, the highest hetero-oligomeric Aβ40 species (hexamers) caused dramatic cell death (Fig 4C). Additionally, cell viability after Aβ treatment was determined on primary hippocampal neurons (Fig 4E). Again the Aβ42 K16N peptide was significantly less harmful than Aβ42 wt, whereas, the mix exhibited similar toxicity as Aβ42 wt (Fig 4E). Noticeably, the Aβ40 mix induced substantial cell loss compared to the non-toxic Aβ40 wt or K16N peptides (Fig 4E). Based on this data we conclude that Aβ42 K16N peptides *per se* are much less toxic than Aβ42 wt, but gain considerable toxicity when mixed with wt peptides. Therefore, we asked why the Aβ mix becomes severely toxic. To visualize the hetero-oligomeric state, we generated a structural model of Aβ wt and K16N hetero-tetramers on the basis of the Aβ42 structure (Luhrs et al, 2005; Fig 4F). In this model hydrogen bonds between the side chains of neighboring K16 and N16 residues locally stabilize the β-sheet conformation, an interaction, that is absent in the WT peptides. The additional hydrogen bond would lend increased stability to the heteromers, which

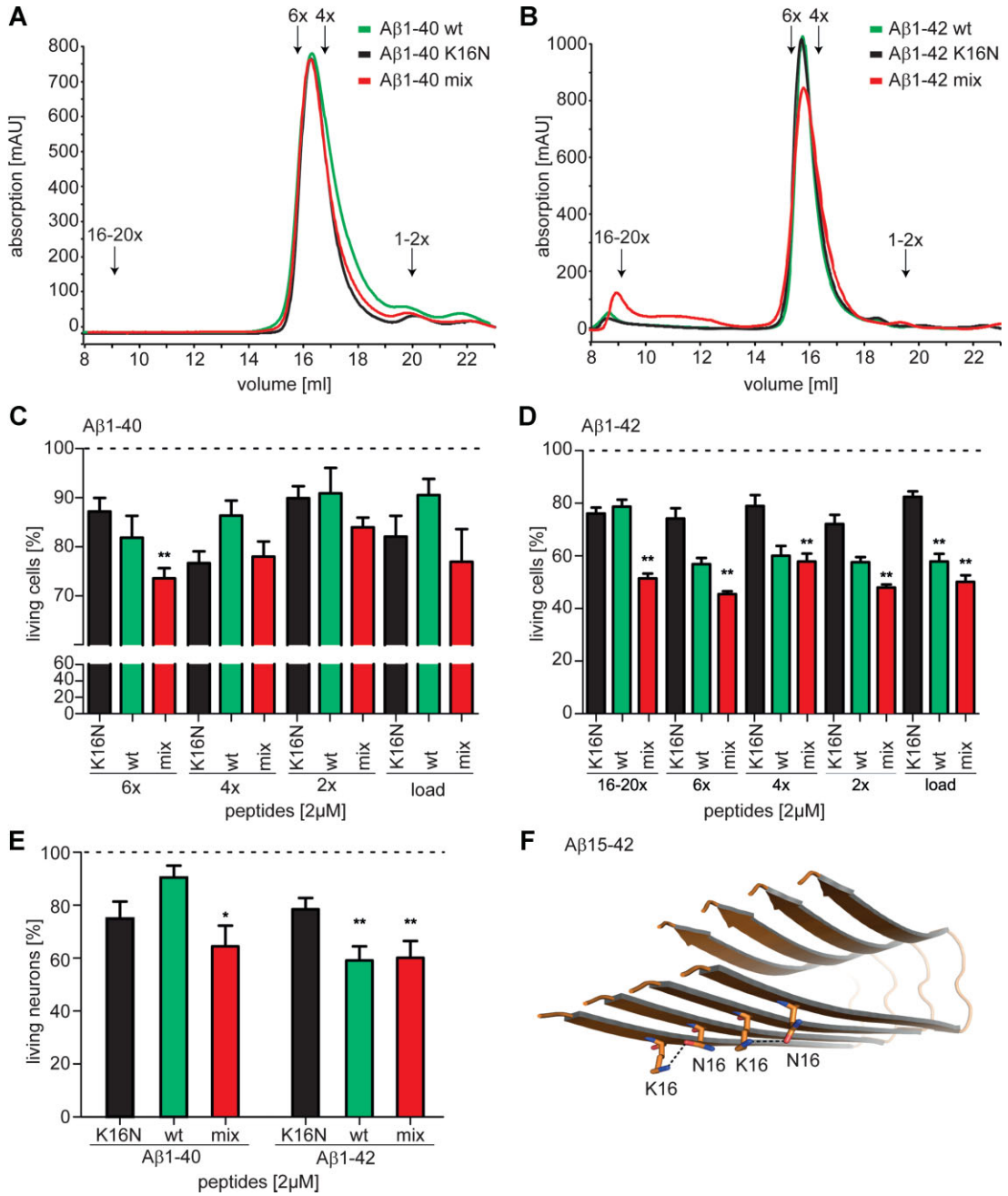

Figure 4. Oligomerization and toxicity of K16N-substituted Aβ peptides.

A,B. SEC of freshly dissolved Aβ40 or Aβ42 wt (green), K16N (black) and the equimolar mixture of both peptides (mix, red). The chromatograms show all similar distributions of low molecular weight oligomers. Note that in the Aβ42 mix, the oligomer distribution shifted from low-*n* oligomers (4–6x) to high-*n* oligomers (16–20x).

C,D. SH-SY5Y cells were incubated for 12 h with either 2 μM freshly dissolved peptides (load) or oligomers (2–20x) obtained by SEC.

E. Primary hippocampal neurons were incubated for 48 h with 2 μM freshly dissolved peptides. In **C–E** toxicity was determined by percentage of living cells compared to untreated control cells ($n = 4$–8 +SEM). One-way ANOVA, Bonferroni's multiple comparison test ($^{*}p < 0.001$ and $^{**}p < 0.0001$).

F. Tertiary structure model for Aβ1–42 mix (wt + K16N) tetramer based on the solution NMR structure Luhrs et al (2005) (see methods). In this model, K16 and N16 form a 2.0 Å short, and thus presumably strong, inter-strand hydrogen bond (black dots). The side chains of K16 and N16 are depicted as sticks, with the nitrogen and oxygen atoms in red and blue, respectively.

might be reflected by the shift to 16–20-mers in the Aβ42 mix by SEC. These stabilized heteromeric structures could account for the modulation of aggregation and toxicity of the Aβ42 mix.

When analysing the fibrillization we found that only Aβ42 wt but neither Aβ40 wt nor the mutant peptides (Aβ40 K16N and Aβ42 K16N) formed rigid mature fibrils as visualized by electron micrographs of 24 h-aged samples (Fig 5A). Aggregates of Aβ40 and Aβ42 K16N deposit in random globular structures. Mixing wt and K16N peptides in an equimolar ratio and thereby mimicking the assumed *in vivo* situation, we observed an inhibition of mature fibril formation in favour of protofibrillar aggregates (Fig 5A).

This data and the strongly increased Aβ levels prompted us to investigate the stability of Aβ42 peptides against clearance activity such as cleavage by NEP, one of the major Aβ-degrading enzymes (Carson & Turner, 2002). We co-incubated freshly dissolved synthetic Aβ42 peptides (wt, K16N, E22G and the respective equimolar mixtures wt/K16N, wt/E22G and K16N/E22G) with human NEP for 6 h and analysed Aβ42 levels by Western blot analysis (Fig 5B). Intensities of bands representing Aβ42 K16N monomers were much higher compared with Aβ42 wt or E22G even in the equimolar mixtures. This indicates a higher stability of Aβ42 K16N peptides against NEP proteolysis. To characterize the proteolytic fragments generated by NEP we carried out MALDI-MS analysis (Fig 6). Proteolysis of the Aβ42 wt peptide by NEP resulted in the generation of the following fragments: 4–9, 12–17, 10–16, 1–9, 10–17 (Fig 6A), 1–16 and 1–17 (Fig 6B). A comparable pattern was observed for Aβ42 E22G (Fig. 6). When digesting Aβ42 K16N with NEP we generally found a decreased amount of proteolytic peptides, which is in line with the higher residual amount of Aβ 1–42 as seen in Fig 5B. However, we clearly detected the peptides 4–9 and 1–9 (Fig 6A). Aβ12–17 and 10–16 K16N were decreased and Aβ10–17 was hardly seen (Fig 6A). In addition, Aβ1–17 K16N was clearly absent and Aβ1–16 K16N strongly reduced (Fig 6B). Hence, Aβ42 K16N is indeed partly resistant to degradation by NEP especially at positions 16 and 17. Interestingly, cleavage directly after residue 16 is possible though at a lower level, although, this is the position of substitution.

DISCUSSION

Our data indicates that the APP K16N mutation has more than one property to render it pathogenic. This can be concluded from two lines of investigation to characterize the mutation (i) APP processing and (ii) properties of the mutated peptide, that is toxicity, aggregation and stability. While the effects as discussed below suggest the possibility that this novel mutation is pathogenic, the genetic support is inconclusive. According to the criteria discussed by Guerreiro et al the mutation can be classified as possible pathogenic (Guerreiro et al, 2010). According to the strong functional data, however, the evidences are in favour to classify this mutation as probable pathogenic. Nevertheless, additional cases from other investigations will be needed to classify this mutation as definitively pathogenic (Guerreiro et al, 2010).

APP processing

The drastically reduced amount of sAPPα which possesses a neuroprotective activity (Furukawa et al, 1996) implies that the

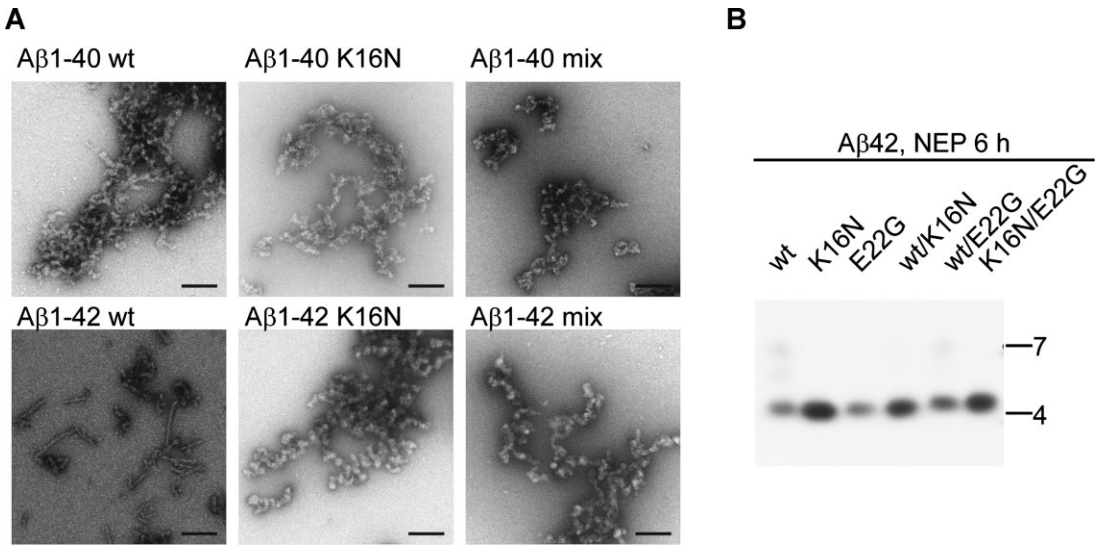

Figure 5. Fibril formation of K16N-substituted Aβ peptides and stability of Aβ42 peptides.

A. Aggregation properties of Aβ wt and K16N peptides. Electron micrographs of freshly dissolved Aβ40 or Aβ42 peptides aged for 24 h and negatively stained. Mix indicates equimolar mixtures of wt and K16N peptides. Only Aβ42 wt peptides form long and rigid fibrils, whereas, co-aggregation of wt and K16N peptides leads to the formation of aggregates comparable with K16N alone. Bar 100 nm.

B. Freshly dissolved Aβ42 peptides (wt, K16N, E22G and the respective 1:1 mixes wt/K16N, wt/E22G and K16N/E22G) were incubated for 6 h with human NEP and analysed by Western blot analysis. Aβ was detected by the W0-2 antibody. Aβ42 K16N peptides are more stable against NEP proteolysis.

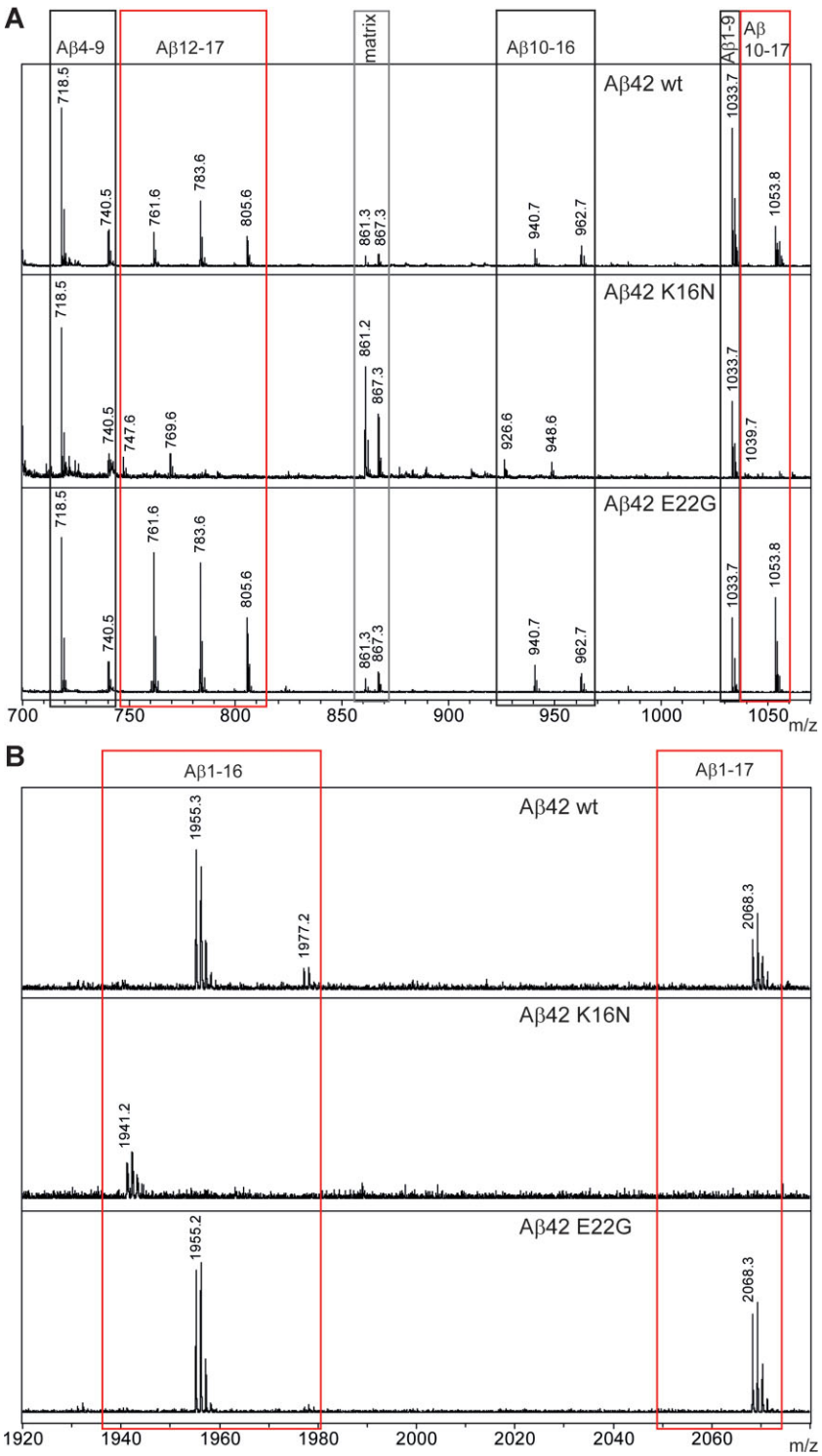

Figure 6. Aβ42 degradation. Mass spectra of NEP proteolysis of Aβ42 peptides (wt, K16N and E22G). Freshly dissolved peptides were incubated for 6 h with human NEP, mixed with α-cyano-4-hydroxycinnamic acid matrix and analysed by MALDI-MS. Peptide identities are indicated at the top. See Table S5 of Supporting Information for the experimental and predicted masses. Aβ42 K16N degradation is strongly inhibited after position L17 and slowed down at position K16.

A. Spectra with mass range from 700 to 1070 Da.

B. Spectra with mass range from 1920 to 2070 Da.

brain capacity for neuroprotection and neurogenesis might be impaired by the expression of APP K16N. Two other mutations which are located at least in close proximity to the α-secretase cleavage site (K16/L17), namely Flemish (A21G) and Arctic (E22G), also show diminished non-amyloidogenic processing (Haass et al, 1994; Sahlin et al, 2007; Stenh et al, 2002). The reduced α-secretase cleavage of APP K16N is attributable to the amino-acid exchange at position 16 as demonstrated by α-secretase *in vitro* assays. However, APP E22G α-cleavage is reduced due to a change in subcellular localization (Sahlin et al, 2007) and, in line with that, comparable to the WT in our *in vitro* assay.

The conundrum that we found sAPPβ levels decreased but amounts of Aβ40 and Aβ42 increased could be solved by the analysis of the respective CTFs generated from APP K16N. While the amount of α-CTF was drastically reduced, levels of β-CTF increased. We propose that increased β-CTF levels are the result of a sequence-specific inhibition of the secondary α-secretase cleavage of the β-CTF. From our results we roughly estimate that usually one half of the β-CTF is subjected to a secondary cleavage by the α-secretase and thus one fourth of α-CTF is generated from β-CTF. A similar high increase in β-CTF was observed when the α-secretase ADAM10 was knocked down in SH-SY5Y cells (Kuhn et al, 2010). This implies that the less β-CTF is re-cleaved by the α-secretase, the more Aβ is generated by γ-secretase cleavage. Thus, one possible cause of the high Aβ levels observed might be the strongly diminished α-cleavage of β-CTF which represents a risk factor for augmented Aβ42 generation resulting in pathogenesis.

Properties of the mutant Aβ peptides

Comparable to the known intra-Aβ mutations, K16N also influenced the aggregation propensities and fibril formation of Aβ peptides. In contrast to the other mutant peptides which exhibit similar or more deleterious effects to neurons than Aβ wt (Kumar-Singh et al, 2002; Murakami et al, 2002; Van Nostrand et al, 2001) freshly dissolved Aβ42 K16N peptides alone are almost non-toxic. However, the equimolar mix of Aβ K16N and wt drastically potentiated toxicity. Since the majority of FAD mutations are dominantly inherited and appear in the heterozygous state, this is a remarkable aspect which needs to be considered also for other mutations. Interestingly and supporting this hypothesis, the mix of wt and mutant Aβ peptides with the recessive A673V (A2V, according to Aβ numbering) mutation was protective *in vitro* and *in vivo* (Di Fede et al, 2009). Therefore, it is tempting to speculate that other than A673V carriers which are only affected in the homozygous state but remain healthy in the heterozygous state, homozygous K16N carriers would not develop early onset dementia. The fact that on the molecular level a crosstalk between wt and K16N Aβ42 peptides is required for toxicity shows that intermolecular contacts involving K16 and N16 cause generation of the toxic species. Even more, it is remarkable that the crosstalk between K16N and wt results in toxic hexamers of the Aβ40 mix. Therefore, we suggest that the stabilization of the β-sheet through an intermolecular amide–hydrogen bond between wt K16 and mutant N16 might induce and stabilize a toxic conformation of Aβ40 and Aβ42. The cellular mechanism of Aβ-mediated toxicity and the nature of the toxic agent associated with pathogenesis (*e.g.* oligomeric form, interaction partners) have remained unclear up to today. However, the existence of non-toxic low-*n* oligomers (Harmeier et al, 2009) and toxic high-*n* oligomers described here indicates that toxicity and oligomerization are not *sine qua non* to each other. Furthermore, mixing Aβ42 wt and K16N peptides inhibited fibril formation of Aβ42 wt which might be indicative for a higher stability of oligomeric species. These stable and toxic hetero-oligomers most probably cause toxicity over a longer period of time which is another important risk factor for the pathogenesis.

For the Aβ40 A21G peptide it has been shown that NEP-mediated degradation is attenuated, whereas, the other intra-Aβ mutations did not affect degradation by NEP (Betts et al, 2008). Here we analysed NEP degradation of Aβ42 peptides and corroborated that wt and arctic peptides are degraded by NEP equally well (Betts et al, 2008). The Aβ K16N peptide, however, was much less efficiently degraded by NEP. This was evident from a higher level of the full-length peptides and the complete loss of Aβ1–17 fragments. Even in the equimolar mixtures of Aβ42 wt/K16N and K16N/E22G the amounts of Aβ42 were higher than in wt and E22G alone. However, we cannot determine whether this increase is only due to the enhanced amounts of Aβ42 K16N or whether Aβ42 wt and E22G were protected from degradation through the physical interaction with Aβ42 K16N.

The mechanism underlying the K16N mutation is novel as it combines different risk factors apparently resulting in early onset dementia. Risk factor one is the higher amount of Aβ peptides due to the K16N mutation affecting APP processing, for example increasing the level of the γ-secretase substrate β-CTF and reducing the levels of neuroprotective sAPPα. In contrast to the arctic mutation, reduced α-cleavage is directly attributable to the amino-acid substitution and not to secondary factors such as localization. Risk factor two is the hetero-oligomer formation of the Aβ K16N peptide with its WT counterpart which severely increases toxicity, especially of the usually non-toxic oligomers. Risk factor three is the change in fibril formation of the Aβ42 K16N peptides. The inhibition of Aβ42 wt fibril formation by Aβ42 K16N renders the toxic heteromeric oligomers more stable and leaves them present over a longer time period. Risk factor four is that Aβ42 K16N peptides are protected against clearance activity by the major Aβ-degrading enzyme NEP which in addition leads to a higher level and an extended half-life of toxic oligomers. Although, we cannot clearly classify the factors according to their importance *in vivo*, every factor alone might be sufficient to increase the risk of getting dementia and, in combination, to cause early onset dementia.

MATERIALS AND METHODS

Molecular-genetic diagnostics

We sequenced genomic PCR products of exons 16 and 17 of APP, the 10 coding exons of PSEN1 and PSEN2, respectively, and the coding exon of PRNP of the index patient. SNPs rs429358 and rs7412 in exon 4 of APOE were genotyped from another genomic PCR product of the patient by melting curve analysis of allele-specific hybridization probes. After appropriate genetic counselling, informed consent from the patient and her husband was given for the genetic and molecular analysis including publication of the data.

Clinical-laboratory analysis of CSF

Aβ42, total tau and phospho-tau$_{(181P)}$ were analysed by commercially available INNOTEST® solid-phase enzyme immunoassays according to the manufacturer's instructions (Innogenetics). CSF samples were obtained from the biomaterial bank of the 'Alzheimerforschergruppe Hamburg' granted by the Deutsche Forschungsgemeinschaft (DFG). CSF samples were obtained at the Memory Clinic of the Department of

Psychiatry and Psychotherapy of the University of Hamburg Medical Center-Eppendorf using standard lumbar-puncture procedure and were immediately aliquoted, stored on dry ice, frozen at −80°C within 30 min and thawed directly before experimental procedure. Informed consent according to the Declaration of Helsinki was obtained before donation of CSF samples from each study participant. Biosampling and study procedures were approved by the local Ethical Committee.

Plasmids

The pcDNA3-APP-YFP and CFP fusion vectors that were used for microscopy have previously been described (Munter et al, 2007). For all other transfections, we used the pcDNA3.1/Zeo (Invitrogen) vector containing APP695. APP695 was N-terminally fused to a myc tag which was inserted after the signal peptide at amino acid position 21. Protein sequence after the myc tag continues with amino acids 20 and 21 (VP). The APP K16N point mutation (position K687 in APP770) was introduced in the three expression vectors by site-directed mutagenesis according to the manufacturer's protocol (Stratagene). The following primers were used: MP-APP-K612N: GAAGTTCATCATCAAAACTTGGTGTTCTTTGCAGAAGATGTGGG and MP-APP-K612N-R: CCACATCTTCTGCAAAGAACACCAAGTTTTGATGATGAACTTC. All expression vectors were verified by DNA sequencing (GATC, Germany).

Cell culture and transfections

SH-SY5Y cells (ATCC number: CRL-2266) were cultured in 1:1 Ham's-F12/DMEM (Biochrom) with 10% FCS (PAA), 2 mM glutamine (PAA) and non-essential amino acids (PAA) and plated at a cell density of 4×10^5 cells per well of a 12-well dish. For transient expression of APP constructs, plasmids (1.5 μg) were incubated in 200 μl Optimem (Invitrogen) with 2 μl Transfectine (BioRad) for 30 min and transferred to the cells. HEK293 cells were cultured in DMEM/high glucose (PAA) with 10% FCS (PAA) and plated at a cell density of 4GATC10^5 cells per well of a 12-well dish (or 6GATC10^5 cells per well of a 6-well plates for cell surface biotinylation). For transient transfections 1.5 μg (3 μg) DNA and 1.5 μl (3 μl) polyethyleneimine (Sigma) were mixed thoroughly in 200 μl (400 μl) Optimem (Invitrogen) and incubated for 30 min before adding to the cells. For ELISA, the medium of cells was replaced by 500 μl fresh Optimem prior to transfection, given a final volume of 700 μl. All transfected cells were incubated for 12 h. Cell surface biotinylation was performed by using EZ Link sulfo-NHS-SS-biotin (Pierce) as previously described (Kaden et al, 2009). To block protein synthesis, cells were treated with 300 μl Optimem containing 10 μg/ml CHX (Sigma Aldrich) or vehicle (DMSO, Sigma), GM6001 (Calbiochem) or BACE inhibitor IV (Calbiochem) for up to 4 h.

Sandwich ELISA

Aβ40/Aβ42 ELISAs were performed according to the manufacturer's instructions (TGC, Zürich). For detection of sAPPα, we used an anti-Myc antibody (Cell Signaling Technology) and W0-2-Biotin (TGC). W0-2-Biotin was recognized by streptavidin-conjugated HRP, ELISAs were developed with 1-Step-Ultra-TMB (Pierce), and measured at 450 nm in a microplate reader (Anthos). Every construct was expressed in triplicates for each ELISA measurement.

MALDI-MS of Aβ human CSF and cell culture supernatant

Aβ was immunoprecipitated from human CSF or conditioned cell culture medium. For immunopurification, 50 μl of CSF were diluted in 450 μl PBS and Aβ was precipitated with 3 μg W0-2 coupled to protein-G sepharose (GE Healthcare). Aβ from conditioned medium was precipitated with 5 μg G2-10 antibody (TGC) coupled to protein-G sepharose. Sepharose was washed first in PBS, then with buffer A (10 mM Tris pH 7.5; 150 mM NaCl; 0.2% NP-40; 2 mM EDTA) and buffer B (buffer A with 500 mM NaCl), followed by PBS and finally 100 mM ammonium acetate (pH 7.4) or distilled water. Aβ was eluted twice with 350 μl of 50% acetic acid and vacuum-dried. The sample was resuspended in 10 μl of 33% acetonitrile containing 0.1% trifluor acetic acid and ultrasonicated. MALDI-MS analysis was carried out on sinapinic acid matrix with an Ultraflex II TOF/TOF (Bruker Daltonics).

Western blot analysis, immune precipitation and antibodies

Cells were washed with PBS and lysed in 20 mM Tris, pH 7.5, 0.5% Igepal Nonidet P-40, 100 mM NaCl, 50 mM NaF, 1 mM EDTA and 1× Complete protease inhibitor mix (Roche Molecular Biochemicals). Samples were subjected to 8% SDS-PAGE and transferred to nitrocellulose membranes (Macherey-Nagel GmbH & Co. KG, Düren, Germany). Immunodetection was performed using primary antibodies followed by probing with horseradish peroxidase-coupled anti-mouse (1:10,000) or anti-rabbit IgG antibodies (1:10,000; both Promega), respectively. Blots were developed by chemiluminescent detection (ECL). For staining of FL-APP and soluble APP (sAPPtotal) we used a murine anti-myc antibody (1:10,000, Cell Signaling Technology). sAPPα was detected by the monoclonal W0-2 antibody (The Genetics Company, Zürich, Switzerland) and the monoclonal 4B4 antibody (Kuhn et al, 2010) and sAPPβ by a polyclonal anti-human-sAPPβ antibody purchased from IBL, Japan. Calnexin was used as a control and was detected by a monoclonal anti-calnexin antibody (MAB3126, Millipore).

Immunoprecipitation of the APP-CTFs was carried out using the self-made polyclonal APP-C-terminal antibody 27576 (immunization with a synthetic peptide APP 648-695 of APP_{695}, Gerd Multhaup) coupled to protein-A sepharose (GE Healthcare). Lysates were incubated with the antibody over night at 4°C in an overhead shaker and washed three times with PBS and two times with 100 mM ammonium acetate (pH 7.4). CTFs were eluted twice with 350 μl of 50% acetic acid and vacuum-dried. Samples were re-dissolved in 2× sample buffer without reducing agents and subjected to gel electrophoresis on 10–20% Tris Tricin gels (Anamed). 10 μl from the Aβ NEP digestions were separated on 10–20% Tris Tricin gels (Anamed) and after blotting detected using the monoclonal W0-2 antibody.

Toxicity

Toxicity on neuroblastoma cells was determined as previously described (Harmeier et al, 2009). Briefly, SH-SY5Y cells were cultured in 96-well dishes at a cell density of 80%. After 48 h, medium was changed and supplemented with freshly dissolved peptides or SEC fractions, each at 2 μM concentration and incubated for 12 h. Cell viability was determined using the MTT assay. Toxicity against primary hippocampal neurons and cell viability was determined as previously described (Harmeier et al, 2009). Briefly, hippocampi of postnatal day 0 (P0)–P1 Wistar rat pups were cultured on glia cell feeder layers. After 10 d *in vitro*, neuronal cultures were treated with freshly dissolved peptides for another 48 h. Neuronal viability was detected

The paper explained

PROBLEM:

Direct genomic sequencing of APP exons 16 and 17 in a 53-year-old patient with early onset dementia identified a novel mutation in the penultimate codon of exon 16 (g. 278263 A>T; c. 2079 A>T), predicting a lysine-to-asparagine substitution at codon 687 (p. K687N; K16N referring to Aβ). The patient presented with progressive cognitive deficits of various modalities, including dyscalculia, decline of short-term memory, verbal fluency and abilities of visual construction. Cognitive decline was confirmed by DemTect neuropsychologically after a 3-month interval. MRI analysis revealed mild global brain atrophy without focal or vascular lesions. Repeated CSF analysis within a time interval of 8 months suggested Alzheimer-type neurodegeneration with elevated total tau, phospho-tau and reduced Aβ1–42 levels. Family history is highly suggestive of autosomal dominant early onset dementia. Samples of other relatives were not accessible for evaluation. Genetic information is nonconclusive in determination of the pathogenicity. Our work unravelled the possible pathogenic mechanisms of the novel APP mutation by functional analysis.

RESULTS:

The novel K16N mutation is located exactly at the α-secretase cleavage site and reduces α-secretase processing *in vitro* and in cell culture. Furthermore, Aβ levels were elevated which is mainly due to reduced secondary cleavage of the β-CTF by the α-secretase. Remarkably, Aβ42 peptides with a K16N substitution were almost non-toxic to neuronal cells, which is in sharp contrast to its WT counterpart. However, when we mixed wt and K16N peptides in an equimolar ratio, and, thereby, mimicked the estimated *in vivo* situation, the mix became severely toxic. Furthermore, Aβ42 K16N inhibited fibril formation of Aβ42 wt. In addition, we found that Aβ42 K16N peptides are more resistant against NEP-mediated degradation.

IMPACT:

The novel mutation we have characterized here harbours an unusual combination of risk factors which may synergistically contribute to the development of early onset AD and has never been described before. The meaningful mutation, in terms of understanding disease-associated or even disease-inducing mechanisms, is located at the α-secretase cleavage site and affects both, APP processing and Aβ peptide properties. The characteristic of the mutation is that the pathogenic effects of the Aβ peptides were only observed in combination with the WT. The influence of the novel K16N mutation on peptide aggregation nicely illustrates the point which we have earlier brought up, that is that toxicity and oligomerization are not *sine qua non* to each other. This we have concluded from the existence of toxic high-*n* oligomers described here and non-toxic low-*n* oligomers obtained with mutations in the GxxxG aggregation motif within the Aβ sequence (Harmeier et al, 2009). Conclusively, when searching for oligomerization modulators as therapeutic agents for the treatment of AD, these substances must be thoroughly screened to prevent any possible toxicity which might result from a stabilization of toxic oligomeric conformations.

Thus, our work nicely demonstrates how the combination of clinical, cell biological and biochemical methods provides insights in the possible mechanisms of pathogenicity of novel mutations identified in single families when segregation-based evidence is not available.

using the MultiTox-Fluor Multiplex Cytotoxicity assay (Promega), performed according to the manufacturer's instructions.

Peptides

Peptides were purchased from PSL, Heidelberg and verified by matrix-associated laser desorption ionization-mass spectrometry (MALDI-MS; Ultraflex-II TOF/TOF, Bruker Daltonics). Synthetic Aβ11-28 peptides were dissolved in water and used immediately. Aβ40 and Aβ42 peptides were dissolved in 98% formic acid. After immediate evaporation of the solvent, peptides were dissolved to 1 mg/ml in 0.1% ammonia in water (Schmechel et al, 2003).

Size exclusion chromatography (SEC)

SEC was performed as previously described (Harmeier et al, 2009) by using a Superdex 75 (10/30HR) column (GE Healthcare). Aliquots of 0.5–1 mg freshly dissolved synthetic peptides, either wt or the substitution peptide K16N alone or an equimolar mix of both peptides, were loaded, and 1 ml fractions were eluted with 1x PBS (137 mM NaCl, 2.7 mM KCl, 10 mM Na_2HPO_4, 2 mM KH_2PO_4, pH 7.4) at a flow rate of 0.5 ml/min. Peptide concentrations were determined by the BCA assay and the collected fractions were immediately used for subsequent experiments.

Electron microscopy

Each peptide was dissolved to 40 μM in deionized water (MilliQ, Millipore) supplemented with 0.1% ammonia and incubated for 24 h at room temperature. Aliquots (10 μl) of the aged peptides were negatively stained with 2% aqueous uranyl acetate as described (Steven et al, 1988). Micrographs were taken using a Philips CM100 electron microscope at 100 kV and a Fastscan CCD camera (Tietz Video and Image Processing Systems, Gauting, Germany).

ADAM *in vitro* assay

A total of 20 μg/ml of the water dissolved Aβ11–28 peptides (10 μM) were subjected to either 0.4 μg (192 nM) recombinant human ADAM10 (R&D SYSTEMS) or 0.1 μg trypsin as a control and incubated in 40 μl of 25 mM ammonium-bicarbonate buffer supplemented with 2 μM $ZnCl_2$. Samples were incubated at 37°C and at the indicated times co-crystallized with α-cyano-4-hydroxycinnamic acid matrix, spotted on a massive gold target and analysed with an Ultraflex II TOF/TOF (Bruker Daltonics).

Neprilysin *in vitro* assay

A total of 20 μg/ml of the dissolved synthetic Aβ42 peptides (4.5 μM) were incubated with 0.5 μg (155 nM) recombinant human NEP (R&D SYSTEMS) and incubated in 40 μl of 25 mM ammonium-bicarbonate buffer supplemented with 2 μM $ZnCl_2$. Samples were incubated at 37°C and after 6 h 1 μl sample was taken and immediately mixed with α-cyano-4-hydroxycinnamic acid matrix, crystallized on a massive gold target and analysed with an Ultraflex II TOF/TOF (Bruker Daltonics).

Molecular modelling

The NMR structure of Aβ42 (Luhrs et al, 2005) was used to build up a hypothetical model of the N-terminally elongated structure of the Aβ1–42 mix tetramer. In the template NMR structure, K16 directly precedes the structured region (residue 17–42) forming a β-turn-β fold. In the Aβ42 structure the side chains of K16 or N16 are expected to compete with the regular main-chain hydrogen bonding network of the β-sheet. In the Aβ mix model, however, strong hydrogen-bonds between the side chains of neighboring K16 and N16 may stabilize the β-sheet, therefore, residues 12–16 were also added in β-sheet conformation. The model of the tetramer was built using the Swiss PDB viewer and energetically minimized using the GROMOS force field.

For more detailed Materials and Methods see the Supporting Information.

Author contributions

DK and AH contributed equally to this work; GM, UF, DS, DK, AH and MS conceived the study; DK has planned and carried out the experiments on the APP K16N processing; DK and CW conducted and analysed the Aβ proteolysis by ADAM and NEP; AH has designed and conducted the characterization of the Aβ K16N peptide aggregation and toxicity on neuroblastoma cells; AH and BRR analysed the Aβ toxicity on primary neurons; VA did the MALDI-MS analysis of the human CSF; RL and AH recorded and evaluated the electron-microscopy images; PWH provided the tertiary structure model of Aβ42 hetero-tetramers; UF, SS, RY and SA carried out the initial patient anamnesis and provided the patient's material; All authors critically discussed results; DK, AH and LMM wrote the manuscript with critical evaluation by GM.

Acknowledgements

We greatly thank Stefan Lichtenthaler (LMU and DZNE, Munich, Germany) for providing us with the 4B4 antibody. This work was supported by grants from the DFG (SFB740, MU901, GRK1123, Exc 257 NeuroCure) and the Hans and Ilse Breuer Foundation (to VA).

Supporting Information is available at EMBO Molecular Medicine online.

The authors declare that they have no conflict of interest.

References

Betts V, Leissring MA, Dolios G, Wang R, Selkoe DJ, Walsh DM (2008) Aggregation and catabolism of disease-associated intra-Abeta mutations: reduced proteolysis of AbetaA21G by neprilysin. Neurobiol Dis 31: 442-450

Carson JA, Turner AJ (2002) Beta-amyloid catabolism: Roles for neprilysin (NEP) and other metallopeptidases? J Neurochem 81: 1-8

Chen YR, Glabe CG (2006) Distinct early folding and aggregation properties of Alzheimer amyloid-beta peptides Abeta40 and Abeta42: stable trimer or tetramer formation by Abeta42. J Biol Chem 281: 24414-24422

De Jonghe C, Zehr C, Yager D, Prada CM, Younkin S, Hendriks L, Van Broeckhoven C, Eckman CB (1998) Flemish and Dutch mutations in amyloid beta precursor protein have different effects on amyloid beta secretion. Neurobiol Dis 5: 281-286

Di Fede G, Catania M, Morbin M, Rossi G, Suardi S, Mazzoleni G, Merlin M, Giovagnoli AR, Prioni S, Erbetta A, *et al* (2009) A recessive mutation in the APP gene with dominant-negative effect on amyloidogenesis. Science 323: 1473-1477

Furukawa K, Sopher BL, Rydel RE, Begley JG, Pham DG, Martin GM, Fox M, Mattson MP (1996) Increased activity-regulating and neuroprotective efficacy of alpha-secretase-derived secreted amyloid precursor protein conferred by a C-terminal heparin-binding domain. J Neurochem 67: 1882-1896

Guerreiro RJ, Baquero M, Blesa R, Boada M, Bras JM, Bullido MJ, Calado A, Crook R, Ferreira C, Frank A, *et al* (2010) Genetic screening of Alzheimer's disease genes in Iberian and African samples yields novel mutations in presenilins and APP. Neurobiol Aging 31: 725-731

Haass C, Hung AY, Selkoe DJ, Teplow DB (1994) Mutations associated with a locus for familial Alzheimer's disease result in alternative processing of amyloid beta-protein precursor. J Biol Chem 269: 17741-17748

Hardy J (2006) A hundred years of Alzheimer's disease research. Neuron 52: 3-13

Hardy J, Selkoe DJ (2002) The amyloid hypothesis of Alzheimer's disease: progress and problems on the road to therapeutics. Science 297: 353-356

Harmeier A, Wozny C, Rost BR, Munter LM, Hua H, Georgiev O, Beyermann M, Hildebrand PW, Weise C, Schaffner W, *et al* (2009) Role of amyloid-beta glycine 33 in oligomerization, toxicity, and neuronal plasticity. J Neurosci 29: 7582-7590

Howell S, Nalbantoglu J, Crine P (1995) Neutral endopeptidase can hydrolyze beta-amyloid(1–40) but shows no effect on beta-amyloid precursor protein metabolism. Peptides 16: 647-652

Iwata N, Tsubuki S, Takaki Y, Shirotani K, Lu B, Gerard NP, Gerard C, Hama E, Lee HJ, Saido TC (2001) Metabolic regulation of brain Abeta by neprilysin. Science 292: 1550-1552

Iwata N, Mizukami H, Shirotani K, Takaki Y, Muramatsu S, Lu B, Gerard NP, Gerard C, Ozawa K, Saido TC (2004) Presynaptic localization of neprilysin contributes to efficient clearance of amyloid-beta peptide in mouse brain. J Neurosci 24: 991-998

Kaden D, Voigt P, Munter LM, Bobowski KD, Schaefer M, Multhaup G (2009) Subcellular localization and dimerization of APLP1 are strikingly different from APP and APLP2. J Cell Sci 122: 368-377

Kalbe E, Kessler J, Calabrese P, Smith R, Passmore AP, Brand M, Bullock R (2004) DemTect: a new, sensitive cognitive screening test to support the diagnosis of mild cognitive impairment and early dementia. Int J Geriatr Psychiatry 19: 136-143

Kanemitsu H, Tomiyama T, Mori H (2003) Human neprilysin is capable of degrading amyloid beta peptide not only in the monomeric form but also the pathological oligomeric form. Neurosci Lett 350: 113-116

Kennedy JL, Farrer LA, Andreasen NC, Mayeux R, St George-Hyslop P (2003) The genetics of adult-onset neuropsychiatric disease: Complexities and conundra? Science 302: 822-826

Klein WL, Krafft GA, Finch CE (2001) Targeting small Abeta oligomers: The solution to an Alzheimer's disease conundrum? Trends Neurosci 24: 219-224

Kuhn PH, Wang H, Dislich B, Colombo A, Zeitschel U, Ellwart JW, Kremmer E, Rossner S, Lichtenthaler SF (2010) ADAM10 is the physiologically relevant,

constitutive alpha-secretase of the amyloid precursor protein in primary neurons. EMBO J 29: 3020-3032

Kumar-Singh S, Julliams A, Nuydens R, Ceuterick C, Labeur C, Serneels S, Vennekens K, Van Osta P, Geerts H, De Strooper B, *et al* (2002) *In vitro* studies of Flemish, Dutch, and wild-type beta-amyloid provide evidence for two-staged neurotoxicity. Neurobiol Dis 11: 330-340

Kuperstein I, Broersen K, Benilova I, Rozenski J, Jonckheere W, Debulpaep M, Vandersteen A, Segers-Nolten I, Van Der Werf K, Subramaniam V, *et al* (2010) Neurotoxicity of Alzheimer's disease Abeta peptides is induced by small changes in the Abeta42 to Abeta40 ratio. EMBO J 29: 3408-3420

Luhrs T, Ritter C, Adrian M, Riek-Loher D, Bohrmann B, Dobeli H, Schubert D, Riek R (2005) 3D structure of Alzheimer's amyloid-beta(1–42) fibrils. Proc Natl Acad Sci USA 102: 17342-17347

Morelli L, Llovera R, Gonzalez SA, Affranchino JL, Prelli F, Frangione B, Ghiso J, Castano EM (2003) Differential degradation of amyloid beta genetic variants associated with hereditary dementia or stroke by insulin-degrading enzyme. J Biol Chem 278: 23221-23226

Munter LM, Voigt P, Harmeier A, Kaden D, Gottschalk KE, Weise C, Pipkorn R, Schaefer M, Langosch D, Multhaup G (2007) GxxxG motifs within the amyloid precursor protein transmembrane sequence are critical for the etiology of Abeta42. EMBO J 26: 1702-1712

Murakami K, Irie K, Morimoto A, Ohigashi H, Shindo M, Nagao M, Shimizu T, Shirasawa T (2002) Synthesis, aggregation, neurotoxicity, and secondary structure of various A beta 1–42 mutants of familial Alzheimer's disease at positions 21–23. Biochem Biophys Res Commun 294: 5-10

Nilsberth C, Westlind-Danielsson A, Eckman CB, Condron MM, Axelman K, Forsell C, Stenh C, Luthman J, Teplow DB, Younkin SG, *et al* (2001) The 'Arctic' APP mutation (E693G) causes Alzheimer's disease by enhanced Abeta protofibril formation. Nat Neurosci 4: 887-893

Portelius E, Westman-Brinkmalm A, Zetterberg H, Blennow K (2006) Determination of beta-amyloid peptide signatures in cerebrospinal fluid using immunoprecipitation-mass spectrometry. J Proteome Res 5: 1010-1016

Sahlin C, Lord A, Magnusson K, Englund H, Almeida CG, Greengard P, Nyberg F, Gouras GK, Lannfelt L, Nilsson LN (2007) The Arctic Alzheimer mutation favors intracellular amyloid-beta production by making amyloid precursor protein less available to alpha-secretase. J Neurochem 101: 854-862

Schmechel A, Zentgraf H, Scheuermann S, Fritz G, Pipkorn R, Reed J, Beyreuther K, Bayer TA, Multhaup G (2003) Alzheimer beta-amyloid homodimers facilitate A beta fibrillization and the generation of conformational antibodies. J Biol Chem 278: 35317-35324

Selkoe DJ (2001a) Alzheimer's disease results from the cerebral accumulation and cytotoxicity of amyloid beta-protein. J Alzheimers Dis 3: 75-80

Selkoe DJ (2001b) Alzheimer's disease: genes, proteins, and therapy. Physiol Rev 81: 741-766

Shirotani K, Tsubuki S, Iwata N, Takaki Y, Harigaya W, Maruyama K, Kiryu-Seo S, Kiyama H, Iwata H, Tomita T, *et al* (2001) Neprilysin degrades both amyloid beta peptides 1–40 and 1–42 most rapidly and efficiently among thiorphan- and phosphoramidon-sensitive endopeptidases. J Biol Chem 276: 21895-21901

Stenh C, Nilsberth C, Hammarback J, Engvall B, Naslund J, Lannfelt L (2002) The Arctic mutation interferes with processing of the amyloid precursor protein. Neuroreport 13: 1857-1860

Steven AC, Trus BL, Maizel JV, Unser M, Parry DA, Wall JS, Hainfeld JF, Studier FW (1988) Molecular substructure of a viral receptor-recognition protein. The gp17 tail-fiber of bacteriophage T7. J Mol Biol 200: 351-365

Van Broeckhoven C, Haan J, Bakker E, Hardy JA, Van Hul W, Wehnert A, Vegter-Van der Vlis M, Roos RA (1990) Amyloid beta protein precursor gene and hereditary cerebral hemorrhage with amyloidosis (Dutch). Science 248: 1120-1122

Van Nostrand WE, Melchor JP, Cho HS, Greenberg SM, Rebeck GW (2001) Pathogenic effects of D23N Iowa mutant amyloid beta-protein. J Biol Chem 276: 32860-32866

Walsh DM, Klyubin I, Fadeeva JV, Cullen WK, Anwyl R, Wolfe MS, Rowan MJ, Selkoe DJ (2002) Naturally secreted oligomers of amyloid beta protein potently inhibit hippocampal long-term potentiation *in vivo*. Nature 416: 535-539

Yang HC, Chai X, Mosior M, Kohn W, Boggs LN, Erickson JA, McClure DB, Yeh WK, Zhang L, Gonzalez-DeWhitt P, *et al* (2004) Biochemical and kinetic characterization of BACE1: investigation into the putative species-specificity for beta- and beta'-cleavage sites by human and murine BACE1. J Neurochem 91: 1249-1259

Younkin SG (1998) The role of Abeta 42 in Alzheimer's disease. J Physiol Paris 92: 289-292

